EEET ECOLOGICAL ENGINEERING & ENVIRONMENTAL TECHNOLOGY

Ecological Engineering & Environmental Technology 2024, 25(5), 265–273
https://doi.org/10.12912/27197050/186182
ISSN 2719-7050, License CC-BY 4.0

Received: 2024.02.20
Accepted: 2024.03.21
Published: 2024.04.01

Performance Enhancement of Polyethersulfone-Based Ultrafiltration Membrane Decorated by Titanium Dioxide Nanoparticles for Dye Filtration

Ihal A. Abed[1], Basma I. Waisi[1*]

[1] Department of Chemical Engineering, College of Engineering, University of Baghdad, Baghdad, Iraq
* Corresponding author's e-mail: basmawaisi@coeng.uobaghdad.edu.iq

ABSTRACT

This study describes the modification of a polyethersulfone (PES)-based membrane by embedding titanium dioxide (TiO_2) nanoparticles. The prepared composite membranes are then characterized and applied for melechate green dye (MG) filtration from water to asses its filtering capabilities. The effect of TiO_2 contents on the morphology and filtration performance of the prepared composite membranes was evaluated by Fourier transform infrared (FTIR), scanning electron microscopy (SEM) and atomic force microscopy (AFM) analysis. The blended membranes displayed improved water permeability and dye rejection compared to the plain PES. The membrane characterization results showed that compared to the plain PES membrane, the porosity of pure membrane increased (from 15.1% to 34.7%) with increasing the percentage of the embedded TiO_2. Then, the optical performance of the prepared membranes was examined in a cross-flow filtration system to separate MG dye from water. The filtration experiments showed that the composite PES/TiO_2 membrane of 1.5 wt.% TiO_2 has the best separation performance (permeate flux of 45 L/m^2.hr and dye removal efficiency of 80%)

Keywords: composite UF membrane, PES polymer, dye removal, TiO_2 nanoparticles, water flux.

INTRODUCTION

Industrial wastewater typically contains a diverse array of organic and inorganic contaminants that require treatment prior to being discharged into the environment. The dyes are among the toxic pollutants in the industrial wastewater. The effluents discharged by various industries, including textile, wool, leather, silk, paper, pulp, ink, cosmetics, pharmaceuticals, and food, contain different dyes (Mahmood and Waisi, 2021). The presence of color in wastewater is the first contaminant identified and must be removed before discharging into water bodies or land. Small amounts of dyes significantly affect the visual impact and aesthetic quality of lakes, rivers, and other water bodies, with concentrations below one ppm for specific colors, which also affects water transparency and the solubility of gases. Hence, it is important to identify a successful method for wastewater treatment to remove color from textile effluents (Alkarbouly and Waisi, 2022a). Various methods, including ion exchange, electrocoagulation, adsorption, and membrane separation, have been used to eliminate dyes from wastewater (Mustafa and Al-Nakib, 2013). Adsorption and membrane technologies have become increasingly common treatment methods because of their notable separation efficiency, absence of byproducts, ability to be regenerated, straightforward operations, and relatively low manufacturing costs. The membrane operates as a barrier between two phases, allowing the selective transport of substances from one side to the other (Al-Okaidy and Waisi, 2023). Polymeric membranes, such as ultrafiltration (UF), microfiltration (MF), nanofiltration (NF), and reverse osmosis (RO), have been created and extensively used to meet the demands of separation and purification processes. The UF membranes compared with RO, lower operating pressure with acceptable efficiency. The UF membranes are frequently prepared from different types of polymers, including polysulfone (PSU), cellulose acetate (CA), polyacrylonitrile (PAN), polyvinylidene fluoride (PVDF), and polyethersulfone (PES) (Han et al., 2013; Waisi et al., 2020).

The polymer type is crucial in determining filtration performance (permeate flux and rejection percentage) (Mohammed et al., 2023). Polyether sulfone (PES) is widely used in membrane manufacturing for water treatment because of its physical and chemical properties, such as ease of processable and appropriate thermal stability in various environmental conditions (Mohammed et al., 2020). The main disadvantage of PES-based membranes is their low permeability due to the created fouling on the membrane surface. Increasing the membrane hydrophilicity is considered an excellent method to decrease the fouling on the membrane during filtration without sacrificing the mechanical properties of the membrane (Luo et al., 2009). One widely used strategy for increasing membrane hydrophilicity and fouling resistance is incorporating hydrophilic inorganic nanoparticles and increasing the water permeability (Meng et al., 2013). Several studies have demonstrated that the inclusion of specific types of nanoparticles, such as silica oxide (SiO_2), can enhance the characteristics of the membrane (Waisi et al., 2019), graphene oxide (GO) (Saeedi-Jurkuyeh et al., 2020), ceric oxide (CeO_2) (Fang and Duranceau, 2013) and silver nanoparticle (AgNP) (Sile-Yuksel et al., 2014). Integrating membrane processes and adsorption techniques is a cutting-edge technology for water and wastewater treatment (Hołda and Vankelecom, 2015). Titanium dioxide (TiO_2) possesses distinct characteristics that it is extensively used in removing several toxic dyes through adsorption and photocatalytic processes due to its stability. Characteristics of the substance include biocompatibility, high oxidizing power, non-toxicity, and affordability (Hu et al., 2013). These characteristics make it well-suited for implementation in wastewater treatment, as it demonstrates a significant ability to improve water permeability and reduce fouling. Applying TiO_2 nanoparticles involves the deposition of TiO_2 onto the surface of a membrane and/or its integration into the membrane's structure (Parvizian et al., 2020; Khalaf and Hassan, 2021). In the current study, PES/DMF precursor solution including TiO_2 nanoparticles were successfully used to create composite UF membranes using the phase inversion approach. The casting solution included the TiO_2 nanoparticles in different percentages. The prepared UF membranes was characterized by Fourier transform infrared (FTIR), scanning electron microscopy (SEM), and atomic force microscopy (AFM) analysis. The produced composite membranes were implied for MG dye separation from water using a cross-flow filtration system to investigate the effect of the embedded TiO_2 nanoparticles on the filtration performance of the membrane.

THE EXPERIMENTAL MATERIALS

The materials

The solution for membrane casting is prepared by implementing polyethersulfone, a polymer with a molecular weight of 56,000, which is procured from BASF Corporation in the United States. NN-Dimethylformamide (DMF), with a minimum assay of 99%, was employed as a solvent sourced from Amber Nath 421 501, India. The American company Sky Springer specializes in nanomaterials and has provided titanium oxide nanoparticles with a purity level of 99%. The malachite green dye with the chemical formula C23H26N2Cl was obtained from Sigma-Aldrich, USA.

Synthesis of PES/ TiO_2 composite membranes

The phase inversion technique yielded mixed matrix ultrafiltration membranes of 16 wt.% PES/DMF consisting of (1, 1.5, and 2 wt.%) TiO_2 nanoparticles. Then the composite precursor solution was subjected to magnetic agitation for 6 hours at a temperature of 35 °C. Then, the solution was undisturbed for 24 hours to remove trapped gases. Then, the polymeric casting solution was poured onto a clean glass using a casting Gardner knife (Filmography: film casting doctor blade) with a thickness of 150 μm. The following step was immersing the glass and cast film in the coagulation medium (deionized water). The formed membrane detached from the glass surface to eliminate any residual solvent and floated away. Before testing, the membranes were immersed in deionized water for at least 24 hours. The process temperature remained consistent at 35 °C.

Membrane characterization

The ultrafiltration membrane's composition was determined by analyzing the samples' FTIR spectra, utilizing products manufactured by

PerkinElmer in Australia. The surface roughness of the membrane was assessed using a scanning probe microscope (SPM AA300 Angstrom Advanced Inc., AFM, USA).

The membranes that had been manufactured were divided into little square pieces and affixed to a metal substrate. The membrane surface was examined using a tapping mode, and all measurements were conducted on dehydrated membrane samples under normal atmospheric conditions.

This study used a scanning electron microscope (SEM) from EO Elektronen-Optik-Service GmbH in Germany, to examine the membranes' surface shape. Before the SEM observation, the membranes underwent the following steps: cracking and platinum sputtering. Subsequently, the dried sample of membranes underwent SEM examinations at different magnifications using a voltage of 5.00 kV. The membrane's porosity is a crucial characteristic in several membrane applications, particularly in relation to the separation efficiency of the membranes (Mohammed et al., 2023).

To evaluate the porosity of flat sheet membranes, the weight of each membrane sample was determined, and then it was submerged in distilled water for 1 hour. The sample's weight was measured before and after being immersed in water, known as the dry and wet weights. Using the gravimetric approach to measure the overall porosity (ε), as represented by the following equation, the porosity % of the flat sheet membranes was ascertained (Sabeeh and Waisi, 2022):

$$\varepsilon = \frac{w1 - w2}{A \times T \times d} \times 100 \tag{1}$$

where: A – stands for the square meter effective area of the membrane, $w1$ and $w2$ – for the wet and dry membranes, d – for the water density at 25 °C (998 kg/m^3), and T – for the thickness of the membrane in millimeters. For each test, the results from three independent runs were considered.

Filtration performance test

The performnace of the prepared ultrafiltration membrane performance was evaluated in color removal using cross flow filtration system. The permeability and removal of dye via the membrane were investigated at ambient temperature and transmembrane pressures of 6 bar. The permeate flux was calculated using Equation 2 (Alkarbouly and Waisi, 2022b).

$$F = \frac{V}{A \times t} \tag{2}$$

where: F is the flow rate, V is the penetrating water rate, A is the effective area, and t is the observed time.

Equation (3) determines the rejection rate R (%).

$$R = \frac{Cf - Cp}{Cf} \times 100 \tag{3}$$

where: Cf and Cp refer to the concentrations (mg/L) in the feed and permeate solutions, respectively.

The dye's concentration was assessed by utilizing a UV-visible spectrophotometer.

THE RESULTS DISCUSSION

Membrane characterization

FTIR analysis

The FTIR-ATR spectra of pure PES/DMF membrane and PES:TiO_2 composite membranes (0, 1, 1.5 and 2 wt.%) TiO_2 are shown in Figure 1 (a, b, c, and d), respectively. Pure PES/DMF membrane structure consists of a benzene ring, a sulfone, and an ether bond. Usually the peaks at 1107–1240 cm^{-1} are ascribed as the bands of aromatic ethers and sulfonyl groups of PES. The band at 717 cm^{-1} is due to the C-S groups, while the bands at 1375 cm^{-1} and 1109 cm^{-1} are attributed to the sulfone group. The peaks at 1462 cm^{-1} and at 1472 cm^{-1} are indicative of alkanes. The spectrum revealed a broad band at 3000–3400 cm^{-1}. This band is associated with OH stretching. Also, the analysis of the spectrum of the embedded TiO_2 in the PES membrane exhibits higher intensity bands at 3200–3400 cm^{-1} due to the more OH vibrations that explained by the high affinity of TiO_2 nano-particles entrapped on the surface structure of the PES membrane to water. The strengthening of OH bonds in the TiO_2 entrapped PES membrane is the main factor in the settlement of TiO_2 nano-particles on the membrane structure (Rahimpour et al., 2011; Zhou et al., 2002; Copello et al., 2011).

In addition, the band around 893 cm^{-1} represents the stretching vibration of short Ti-O bonds. Moreover, the peak observed at 1,598.7 cm^{-1} for PES:TiO_2 membrane was found to be shifted from the band given in the literature at 1,674 cm^{-1}. This shift can be ascribed to interactions

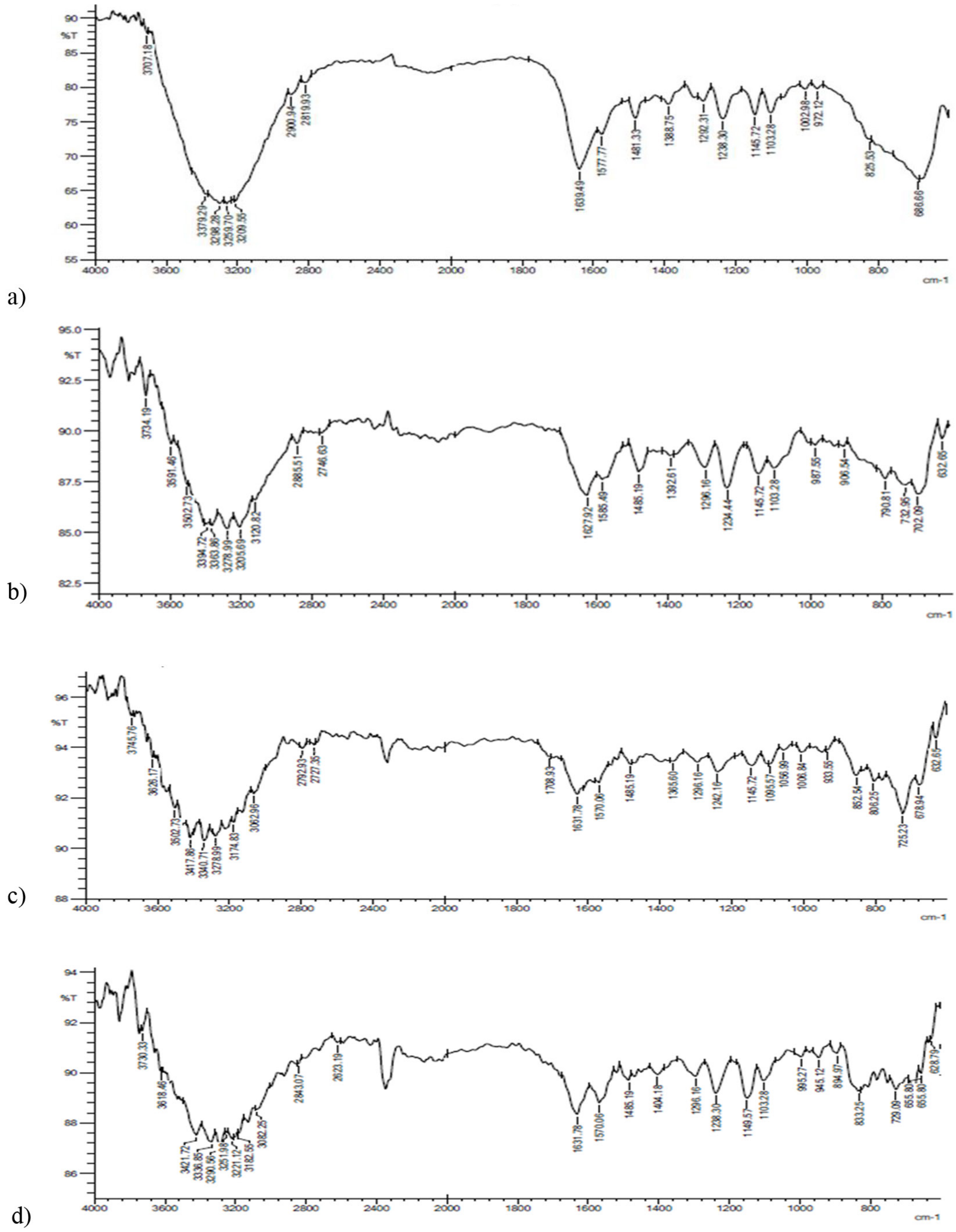

Figure 1. FTIR-ATR spectra of (a) 0%, (b) 1%, (c) 1.5%, and (d) 2% composite UF membranes

of TiO_2 with the sulfone group and ether bond in polyethersulfone structure (Mohamed Shaban et al., 2015). The broad peak around 3500 to 3700 cm^{-1} is augmented the presence of significant amount of OH groups of TiO_2 nanoparticles on membrane surface (Cheshomi, Pakizeh and Namvar-Mahboub, 2018). Scanning electron microscopy images (Figure 2) displays the SEM pictures of the surface morphology of the pure polyether sulfone membrane and its composites with embedded TiO_2. The results indicated that the clean pure PES based membrane has no clear defection or pores on the surface, its porosity was just 30%. Adding the TiO_2 nanoparticles within the membrane matrix results a distinct asymmetric and porous structure, including a significantly semi-dense skin layer, micro voids, and porous, as shown in Figure 2b, c, and d. The surface porosity of the PES:TiO_2 composite membrane increased with embedding 1 and 1.5 wt.% TiO_2 nanoparticles to 33% and 40%. The clear impact of TiO_2 on the surface morphology

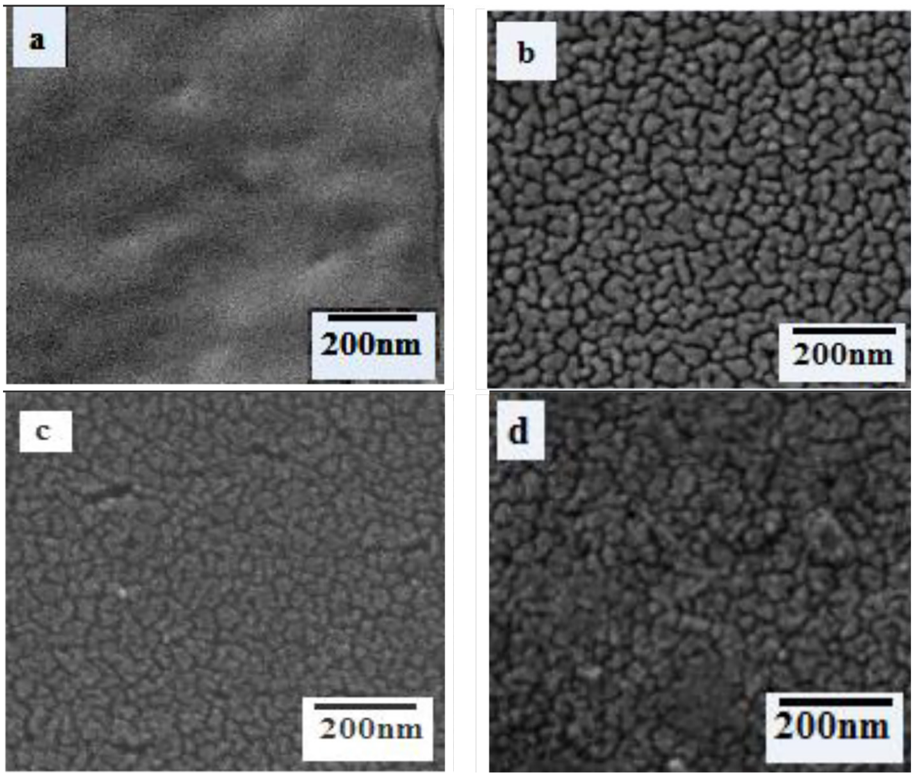

Figure 2. The SEM images of the surface of (a) pure, (b) 1%, (c) 1.5%, (d) 2% composite UF membranes

can be explained by the hydrophilic properties of TiO_2 that can influence the kinetics of the phase separation process, allowing different morphologies to be developed (Luo et al., 2009; Li et al., 2009). This morphology results from the strong attraction between the nonsolvent (water) and the solvent DMF, rapidly separating the phases. Including hydrophilic nanoparticles, such as TiO_2, within the PES layer solution leads to an enhancement in the speed at which mass is exchanged between the underlying layer and the coagulation solution during the phase inversion procedure. This enhancement proves to be beneficial as it promotes the rise in the permeability of the membrane. Thus, it plays an important role in forming large voids and increasing the overall porosity level (Razmjou et al., 2011). the presence of TiO_2 nanoparticles in the casting solution leads to a delay in the mixing of the liquid during the phase inversion process, hence causing an enlargement of the membrane's pore size (Kakar et al., 2015; Ahmad et al., 2017). Further increasing in the TiO_2 nanoparticles showed a slight decrease in the porosity to 37% due to the particles aggregation and the nonuniform distribution of particles within the membrane matrix, as shown in Figure 2d.

Atomic force microscopy images

According to Figure 3, the pure PES/DMF membrane exhibits a rough surface due to the several large peaks and valleys (Ra = 24.81 and Rz = 112.3). Adding the nanoparticles in the mixed matrix membranes alters the surface morphology of the membranes. The addition of 1 wt.% TiO_2 nanoparticles to the PES casting solution results in the formation of membranes with significantly more uneven surfaces compared to the pure PES based membranes (Ra = 32.28 and Rz = 147.5). This phenomenon can be attributed to the dimensions of the TiO_2 aggregates that have developed on the surface of the membrane. Upon blending a higher amount of TiO_2 (1.5%) nanoparticles, the high peaks and valleys were replaced with small ones, leading to the formation of a smoother membrane surface (Ra = 29.54 and Rz = 146.0). The hydroxyl groups of TiO_2 active surface can modify the surface characteristics of nanoparticles that are embedded in the membrane. Several factors can modify the surface properties, including the formation of chain wrinkles, electrostatic interactions among polymer chains, compactness or bending, and variations in the surface area (Esmaeili et al., 2010). Increasing the TiO_2 nanoparticles to

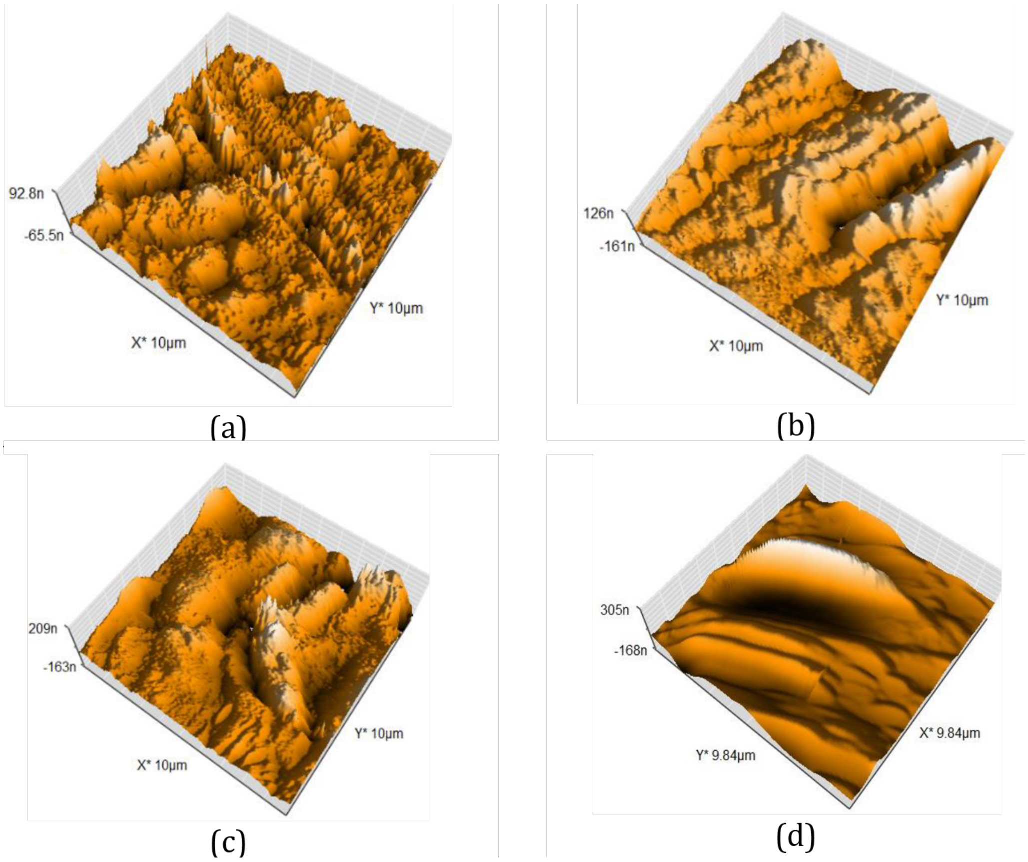

Figure 3. 3D of the AFM images of the PES composite membranes: (a) pure, (b) 1%, (c) 1.5%, (d) 2% composite UF membranes

2%, accumulation of grain spread throughout the membrane surface occurred and resulted in increasing the roughness measure (Sotto et al., 2012; Rajesh et al., 2011).

Performance test

Effect of TiO_2 nanoparticles on the permeability

Figure 4 illustrates the effect of the incorporated TiO_2 within the PES based membrane on the water flux during the MG dye filtration. The pure 16% PES/DMF membrane showed a high flow resistance and did not allow the water to pass through due to the small pores volume.

Table 1. Characterization of membrane surface roughness parameters and porosity

PES-based membrane	Average roughness, Ra (nm)	Mean hight, Rz
Pure PES/DMF	24.81	112.3
1% nano TiO_2	32.28	147.5
1.5% nano TiO_2	29.54	146.0
2% nano TiO_2	46.83	250.2

Embedding 1 wt.% TiO_2 nanoparticles within the PES membrane matrix was not enough to allow the water to pass through the composite membrane. However, increasing the embedded TiO_2 to 1.5 wt.% enhanced the permeate water flow to 48 LMH under a transmembrane pressure of 6 bar. This enhancement with increasing the TiO_2 nanoparticles can be related to the formation of a larger quantity of linked holes and less resistance to water flow. The addition of TiO_2 nanoparticles improved the ability of the membrane to allow substances to pass through by increasing its openness, enlarging the size of its openings, and promoting the creation of specific large empty spaces inside the outer layer. In addition, the presence of hydroxyl groups on the surface of TiO_2 nanoparticles increases the hydrophilicity of the membrane (Saberi et al., 2018); Al-Furaiji et al., 2022). Further increase in the embedded TiO_2 nanoparticle to 2 wt.% resulted in significant declining in the water flux to 23 LMH which can be related to the blocking some of the pores within the membrane by the clumped TiO_2 nanoparticles.

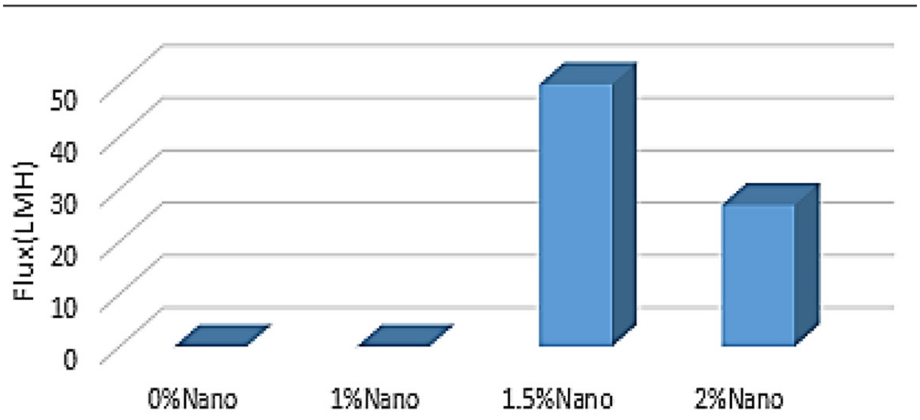

Figure 4. The effect of embedded TiO_2 within PES based membrane on the water flux during the MG dye filtration. The transmembrane pressure of 6 bars and MG dye initial concentration of 10 mg/L

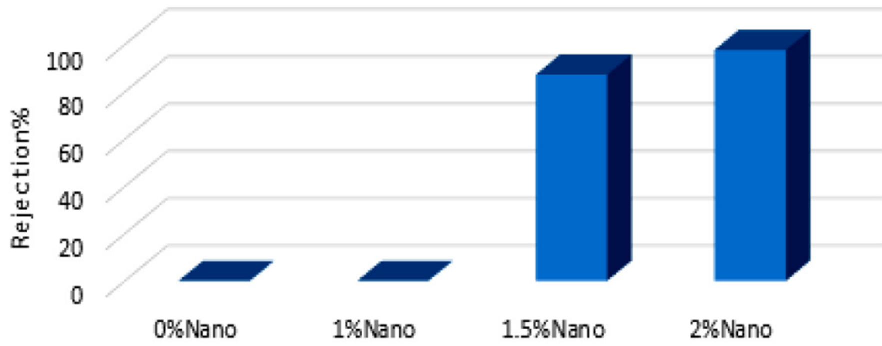

Figure 5. The effect of embedding TiO_2 within PES based membrane on the dye rejection during the MG dye filtration, transmembrane pressure of 6 bars and MG dye initial concentration of 10 mg/L

The effect of TiO_2 NPs on the rejection performance

Figure 5 shows the effect of the added TiO_2 within the PES based membrane on the MG dye rejection during the filtration process. Both of pure PES based membrane and that included 1 wt.% TiO_2 membranes did not allow the water to pass through so the rejection percentage could not be calculated. While the PES:TiO_2 membrane of 1.5 wt.% TiO_2 shows a high rejection percentage 80% of MG dyes because of its developed porous structure. The increased hydrophilicity and lower surface roughness of the 1.5 wt.% TiO_2 membrane probably led to less foulant absorption and superior rejection. Additionally, it is widely known that membranes with greater hydrophilicity are less likely to become fouled (Shoparwe et al., 2018; Al-Bayati et al., 2023; Ahmad et al., 2018). The further increasing in the added TiO_2 concentration to 2 wt.% resulted in increasing the rejection percentage which can be illustrated by the blocked pores on the composite membrane surface due to the agglomeration of TiO_2, as shown previously in the SEM images.

CONCLUSIONS

The PES based membranes and its composite with different concentrations of TiO_2 nanoparticles (1, 1.5 and 2 wt.%) were prepared by phase inversion method then were applied in MG dye separation using a cross-flow filtration system to investigate their filtration performance. SEM pictures showed significant differences in the composite membranes' shape and less dense structure compared to the pristine membrane. These changes were especially apparent on the membrane surface, increasing porosity as the nanoparticle concentration rose. AFM images show that composite membrane surface roughness increases owing to nanoparticle aggregation. The composite membranes' pure water permeability improved with increasing TiO_2 concentrations up to 1 wt.%. Adding 1.5 and 2 wt.% TiO_2 had increased the permeability of water due to the increase in porosity. The composite membranes, including 0 and 1 wt.% TiO_2 showed a slightly reduced in the rejection rates compared to the 1.5 wt.% and 2 wt.% membranes. The composite membrane, with a TiO_2 concentration of 1.5 wt.% and 2 wt.%, showed a very significant rejection rate. Specifically, it achieved a rejection rate of 80 and 95%, respectively, for the Malachite Green dye under a pressure of 6 bar. The composite membrane containing 1.5 wt.% TiO_2 is considered to be an ideal choice for the removal of dyes.

REFERENCE

1. Ahmad, A.L., Abdulkarim, A.A., Shafie, Z.M.H.M., Ooi, B.S. 2017. Fouling evaluation of PES/ZnO mixed matrix hollow fiber membrane. Desalination, 403, 53–63.
2. Ahmad, A.L., Otitoju, T.A., Ooi, B.S. 2018. Optimization of a high performance 3-aminopropyltriethoxysilane-silica impregnated polyethersulfone membrane using response surface methodology for ultrafiltration of synthetic oil-water emulsion. J. Taiwan Inst. Chem. Eng., 93, 461–476.
3. Al-Bayati, I.S., Abd Muslim Mohammed, S., Al-Anssari, S. 2023. Recovery of methyl orange from aqueous solutions by bulk liquid membrane process facilitated with anionic carrier. AIP Conf. Proc., 2414, 1–7. https://doi.org/10.1063/5.0114631
4. Al-Furaiji, M., Waisi, B., Kalash, K., Kadhom, M. 2022. Effect of polymer substrate on the performance of thin-film composite nanofiltration membranes. Int. J. Polym. Anal. Charact., 27, 316–325. https://doi.org/10.1080/1023666X.2022.2073008
5. Al-Okaidy, H.S., Waisi, B.I. 2023. The effect of electrospinning parameters on morphological and mechanical properties of PAN-based nanofibers membrane. Baghdad Sci. J., 20, 1433–1441. https://doi.org/10.21123/bsj.2023.7309
6. Alkarbouly, S.M, Waisi, B.I. 2022a. Fabrication of electrospun nanofibers membrane for emulsified oil removal from oily wastewater. Baghdad Sci. J., 1238–1248.
7. Alkarbouly, S.M., Waisi, B.I. 2022b. Dual-layer antifouling membrane of electrospun PAN: PMMA nonwoven nanofibers for oily wastewater treatment. In: Proceedings of 2nd International Multi-Disciplinary Conference Theme: Integrated Sciences and Technologies., 1–10.
8. Copello, G.J., Mebert, A.M., Raineri, M., Pesenti, M.P., Diaz, L.E. 2011. Removal of dyes from water using chitosan hydrogel/SiO_2 and chitin hydrogel/SiO2 hybrid materials obtained by the sol–gel method. J. Hazard. Mater., 186, 932–939.
9. Fang, Y., Duranceau, S.J. 2013. Study of the effect of nanoparticles and surface morphology on reverse osmosis and nanofiltration membrane productivity. Membranes (Basel), 3, 196–225. https://doi.org/10.3390/membranes3030196
10. Han, B., Zhang, D., Shao, Z., Kong, L., Lv, S. 2013. Preparation and characterization of cellulose acetate/carboxymethyl cellulose acetate blend ultrafiltration membranes. DES, 311, 80–89. https://doi.org/10.1016/j.desal.2012.11.002
11. Hołda, A.K., Vankelecom, I.F.J. 2015. Understanding and guiding the phase inversion process for synthesis of solvent resistant nanofiltration membranes. J. Appl. Polym. Sci., 132, 42130. https://doi.org/10.1002/app.42130
12. Hu, A., Liang, R., Zhang, X., Kurdi, S., Luong, D., Huang, H., Peng, P., Marzbanrad, E., Oakes, K.D., Zhou, Y., Servos, M.R. 2013. Enhanced photocatalytic degradation of dyes by TiO_2 nanobelts with hierarchical structures. J. Photochem. Photobiol. A Chem., 256, 7–15.
13. Kakar, M.R., Hamzah, M.O., Valentin, J. 2015. A review on moisture damages of hot and warm mix asphalt and related investigations. J. Clean. Prod., 99, 39–58.
14. Khalaf, Z.A., Hassan, A.A. 2021. Studying of the effect of many parameters on a bulk liquid membrane and its opposition in Cd(II) removal from wastewater. J. Phys. Conf. Ser. 1973. https://doi.org/10.1088/1742-6596/1973/1/012097
15. Li, J.-F., Xu, Z.-L., Yang, H., Yu, L.-Y., Liu, M. 2009. Effect of TiO_2 nanoparticles on the surface morphology and performance of microporous PES membrane. Appl. Surf. Sci., 255, 4725–4732.
16. Luo, M.L., Wen, Q.Z., Liu, H.J., Liu, J.L. 2009. Effect of TiO_2 nanoparticles on the hydrophilicity of sulfonated-polyethersulfone. In: Advanced Materials Research. Elsevier, 663–666. https://doi.org/10.4028/www.scientific.net/AMR.79-82.663
17. Mahmood, O.A.A., Waisi, B.I. 2021. Synthesis and characterization of polyacrylonitrile based precursor beads for the removal of the dye malachite green from its aqueous solutions. Desalin. Water Treat., 216, 445–455. https://doi.org/10.5004/dwt.2021.26906
18. Mohammed, M.A., Al-bayati, I.S., Alobaidy, A.A., Waisi, B.I., Majeed, N. 2023b. Investigation the efficiency of emulsion liquid membrane process for malachite green dye separation from water. Desalin. Water Treat., 307, 190–195. https://doi.org/10.5004/dwt.2023.29903
19. Mohammed, N.A., Alwared, A.I., Salman, M.S.

2020. Photocatalytic degradation of reactive yellow dye in wastewater using H_2O_2/TiO_2/UV technique. Iraqi J. Chem. Pet. Eng., 21, 15–21. https://doi.org/10.31699/ijcpe.2020.1.3

20. Mustafa, N., Al -Nakib, H. 2013. Reverse osmosis polyamide membrane for the removal of blue and yellow dye from waste water. Iraqi J. Chem. Pet. Eng., 14, 49–55.

21. Parvizian, F., Ansari, F., Bandehali, S. 2020. Chemical engineering research and design oleic acid-functionalized TiO_2 nanoparticles for fabrication of PES-based nanofiltration membranes. Chem. Eng. Res. Des. 156, 433–441. https://doi.org/10.1016/j.cherd.2020.02.019

22. Rajesh, S., Shobana, K.H., Anitharaj, S., Mohan, D.R. 2011. Preparation, morphology, performance, and hydrophilicity studies of poly (amide-imide) incorporated cellulose acetate ultrafiltration membranes. Ind. Eng. Chem. Res., 50, 5550–5564.

23. Razmjou, A., Mansouri, J., Chen, V. 2011. The effects of mechanical and chemical modification of TiO_2 nanoparticles on the surface chemistry, structure and fouling performance of PES ultrafiltration membranes. J. Memb. Sci., 378, 73–84.

24. Sabeeh, H., Waisi, B.I.W. 2022. Effect of solvent type on PAN–based nonwoven nanofibers membranes characterizations. Iraqi J. Chem. Pet. Eng., 23, 43–48. https://doi.org/10.31699/ijcpe.2022.4.6

25. Saberi, S., Shamsabadi, A.A., Shahrooz, M., Sadeghi, M., Soroush, M. 2018. Improving the transport and antifouling properties of poly (vinyl chloride) hollow-fiber ultrafiltration membranes by incorporating silica nanoparticles. ACS Omega, 3, 17439–17446.

26. Saeedi-Jurkuyeh, A., Jafaria, A.J., Kalantary, R.R., Esrafili, A. 2020. A novel synthetic thin-film nanocomposite forward osmosis membrane modified by graphene oxide and polyethylene glycol for heavy metals removal from aqueous solutions. React. Funct. Polym. 146, 104397.

27. Shoparwe, N.F., Otitoju, T.A., Ahmad, A.L. 2018. Fouling evaluation of polyethersulfone (PES)/sulfonated cation exchange resin (SCER) membrane for BSA separation. J. Appl. Polym. Sci., 135, 45854.

28. Sile-Yuksel, M., Tas, B., Koseoglu-Imer, D.Y., Koyuncu, I. 2014. Effect of silver nanoparticle (AgNP) location in nanocomposite membrane matrix fabricated with different polymer type on antibacterial mechanism. Desalination, 347, 120–130. https://doi.org/10.1016/j.desal.2014.05.022

29. Sotto, A., Rashed, A., Zhang, R.X., Martínez, A., Braken, L., Luis, P., Van der Bruggen, B. 2012. Improved membrane structures for seawater desalination by studying the influence of sublayers. Desalination, 287, 317–325.

30. Waisi, B.I., Al-jubouri, S.M., Mccutcheon, R. 2019. Fabrication and characterizations of silica nanoparticle embedded carbon nanofibers. Ind. Eng. Chem. Res., 58, 4462–4467. https://doi.org/10.1021/acs.iecr.8b05825

31. Waisi, B.I., Arena, J.T., Benes, N.E., Nijmeijer, A., McCutcheon, J.R. 2020. Activated carbon nanofiber nonwoven for removal of emulsified oil from water. Microporous Mesoporous Mater., 296, 109966. https://doi.org/10.1016/j.micromeso.2019.109966

32. Zhou, Z.H., Xue, J.M., Chan, H.S.O., Wang, J. 2002. Nanocomposites of $ZnFe_2O_4$ in silica: synthesis, magnetic and optical properties. Mater. Chem. Phys., 75, 181–185.